Rubber Elasticity of Well-Characterized Polybutadiene Networks

Luc M. Dossin and William W. Graessley*

Materials Science and Engineering Department, Northwestern University, Evanston, Illinois 60201. *Received September 28, 1978*

ABSTRACT: Polybutadiene networks in bulk and 50% solution were prepared by radiation-induced cross-linking of well-characterized primary chains. Equilibrium stress–strain behavior was measured in tension, and the initial (small deformation) modulus G_0 as well as the individual Mooney–Rivlin parameters $2C_1$ and $2C_2$ were obtained. The initial modulus was interpreted as the sum of contributions from the chemical network structure G_c and the network topology G_e, the latter trapped in the structure when the network was formed. Within experimental error the maximum topological contribution, G_e^{max}, obtained by the Langley analysis was equal to G_N^0, the stress relaxation plateau modulus prior to cross-linking: G_e^{max} and G_N^0 are 1.18 and 1.16 MPa, respectively, for the undiluted polybutadiene, and 0.262 and 0.243 MPa for 50% solutions. The chemical network contribution in both cases was equal to values calculated from the phantom network theory with junction fluctuations suppressed. The value of $2C_2$ appears to be related in a simple way to the topological contribution. The value of $2C_1$ depends on both the chemical and topological contributions.

The elasticity of rubber networks has been the subject of numerous studies.[1,2] It was realized many years ago that the free energy of deformation has its origin in the configurational free energy of the network strands and that for many purposes the strands can be treated as Gaussian random coils. Subsequent development of these ideas has led to the theory of phantom networks.[3-7] The term "phantom" is used here to emphasize that the configurations available to each strand are assumed to depend only on the positions of its end points and to be otherwise independent of the configurations of neighboring strands.

The theory has been highly successful in a variety of respects. However, stress–strain behavior is frequently found to depart from its predictions. For example, many studies have shown that the observed modulus for small deformations is significantly larger than predicted from the network structure. Various authors have attributed such discrepancies to topological restrictions in real networks. The unperturbed random coil model is now well established for the chain in undiluted amorphous polymers.[8,9] Thus, a great deal of overlap must exist in the domains pervaded by neighboring strands. Chains cannot literally pass through the backbone contours of other chains so the configurations of neighboring strands may very well be conditionally dependent upon one another. Such dependence could produce an additional contribution to the free energy of deformation. The purpose of this paper is to present some results on the topological contribution obtained in randomly cross-linked polybutadiene networks, dealing particularly with its relationship to the plateau modulus of the polymer prior to cross-linking.

The existence of a plateau in the stress–relaxation modulus is a rather general characteristic of long-chain polymer liquids.[10,11] This property has been attributed to chain entanglement, a consequence of the "uncrossability" of chain contours. Rapid relaxation processes involving only local rearrangements of the chain configuration (out to some length which is characteristic of the undiluted polymer) are assumed not to be influenced by the uncrossability of neighboring chains and independent of the total chain length. Slower relaxation processes involving longer portions of the chain are assumed to be strongly retarded and a strong function of total chain length. As a result of this splitting of the relaxation spectrum, the behavior at intermediate times is network-like and characterized by the shear modulus G_N^0. Experimentally, the plateau modulus is independent of chain length for sufficiently long chains and relatively insensitive to temperature. In concentrated solutions G_N^0 is proportional to the square of polymer volume fraction and independent of the nature of the diluent, suggesting a geometrical and pairwise interaction between chain contours.

The plateau modulus is a characteristic constant of the undiluted polymer with values for common species ranging from 0.2 to 2.0 MPa.[10] According to the entanglement interpretation of the topological contribution, a portion of the restrictions on configurational rearrangement become permanently trapped when a network is formed and therefore are able to contribute to equilibrium elasticity.

Polybutadiene has a relatively large plateau modulus (G_N^0 = 1.16 MPa for samples with microstructure similar to those in the present study[10]). Samples of high molecular weight can be prepared, and networks can be formed with large entanglement trapping efficiencies while the modulus calculated from the phantom network theories is still relatively small. Thus, the topological contribution should be rather prominent in this polymer.

Theory for the Small Deformation Modulus

According to the phantom network theory the tensile force per unit unstretched area σ is related to the tensile stretch ratio λ by[6]

$$\sigma = \frac{(\nu - \mu)kT}{V} \frac{\langle r^2 \rangle}{\langle r^2 \rangle_0} (\lambda - 1/\lambda^2) \qquad (1)$$

in which ν and μ are the numbers of elasticity active strands and junctions in the network, V is the network volume, $\langle r^2 \rangle$ is the mean-square end-to-end distance of the strands in the unstretched state, $\langle r^2 \rangle_0$ is the same quantity for the strands with junctions removed, k is the Boltzmann constant, and T is the temperature. A junction is elastically active if at least three of the strands leading away are independently attached to the network; a strand is elastically active if it joins two elastically active junctions.[12a]

In deriving eq 1 it is assumed that the junctions are free to fluctuate about their mean positions. In theories which omit the effect of fluctuations the factor $\nu - \mu$ is replaced by ν alone. It has been suggested recently that configurational involvements with neighboring strands near the junction points may suppress the junction fluctuations to some extent.[7,12b] We can include such an effect empirically by using $\nu - h\mu$ in place of $\nu - \mu$, where the parameter h varies from 0 (complete suppression) to 1 (no suppression). In perfect tetrafunctional networks $\nu = 2\mu$, so the phantom network contribution may vary by as much as a factor of 2, depending on h.

We will restrict ourselves throughout to elastic properties measured with the network occupying the same volume (or nearly so) as when it was formed. Swelling or con-

0024-9297/79/2212-0123$01.00/0

Table I
Molecular Characterization Data

sample	double bond microstructure, % cis (1,4)	trans (1,4)	vinyl (1,2)	$\bar{M}_w$ (GPC) × 10^{-3}	$\bar{M}_w/\bar{M}_n$ (GPC)	$[\eta]_{THF}$	$\bar{M}_n$ (Osm.) × 10^{-3}	$\bar{M}_w$ (L.S.) × 10^{-3}
PB022	40	51	9	22.6	<1.1	0.43	20	18
PB096				96	<1.1	1.25		
PB168	47	45	8	168	<1.1	1.85	155	157
PB210				210	<1.1	2.20		
PB344	55	38	7	344	<1.1	3.32	295	365
PB725				725	<1.1	6.48	700	790

traction from the as-formed state are network deformations in themselves, and, although the network topology is fixed, we have no way to know a priori how such deformations will alter its contribution to the modulus. We assume that $\langle r^2 \rangle = \langle r^2 \rangle_0$ when the network occupies its as-formed volume and the temperatures of network formation and modulus measurement are the same.

To evaluate the topological contribution we will deal mainly with elastic behavior at small deformations. Interpretation should be least ambiguous when the network is relatively undisturbed by the measurement. The initial modulus, given by

$$G_0 = \lim_{\lambda \to 1} \left(\frac{\sigma}{\lambda - 1/\lambda^2} \right) \tag{2}$$

is equal to the small deformation shear modulus (Poisson's ratio $\approx 1/2$). The phantom network value, specialized to the case here, is the chemical network contribution:

$$G_c = \frac{(\nu - h\mu)kT}{V} \tag{3}$$

We will follow others[10] in assuming that the chemical and topological contributions are additive and further that the topological contribution G_e can be written as the product of a maximum possible modulus G_e^{max} and a trapping factor T_e, the fraction of this maximum value actually obtained:

$$G_0 = G_c + G_e^{max} T_e \tag{4}$$

Langley[13] proposed that T_e is the fraction of entanglements trapped when the network was formed and that it should be equal to the probability that all four paths leading away from an entanglement site between two chains lead independently to the network. The idea can be expressed with a less specific molecular picture as follows. Suppose G_e^{max} involves only pairwise geometrical relationships between units on different chains. Let G_e be the sum of contributions from those relationships which are rendered permanent when the network is formed. Permanence means that the strands which contain the two units are each elastically active, so that both units are parts of closed loops within the network. In either interpretation T_e is simply the square of the probability that both paths leading from a randomly selected chain unit join the network.[13] It is also equal to the square of the fraction of chain units which belong to elastically active strands.

To apply the above approach it is necessary to determine ν, μ, and T_e for the networks by a method which does not involve elastic measurements. We will use the gel curve method of Langley and Polmanteer.[14] Samples of known molecular weight distribution are cross-linked by high-energy radiation and the gel fraction is determined as a function of radiation dose. The proportionality constants relating extents of the radiation-induced reactions and dose are determined from the gel curves by applying random-linking theory. With these results the values of ν, μ, and T_e are calculated, again on the basis of the random-linking assumption. Thus, all quantities which govern the initial modulus are predictable except the parameters h ($0 < h < 1$), which may in principle vary from one network to another, and G_e^{max}, which should be the same for all networks formed at the same volume fraction of polymer. If junction fluctuations are suppressed h is zero; G_e^{max} should correspond with G_N^0 if the topological contribution is governed by the same interactions responsible for the relaxation modulus plateau in the polymer before cross-linking.

Experimental Section

Polymer Preparation and Characterization. Linear polybutadiene samples of narrow distribution were prepared by anionic polymerization in cyclohexane at 50 °C. The initiator was *sec*-butyllithium; isopropyl alcohol was used to terminate the reaction. The polymers were precipitated, washed in methanol containing an antioxidant (Santanox R), then stored in a refrigerator.

The double bond composition of some samples was determined by infrared spectroscopy. The observed 7–9% vinyl content (Table I) is typical of polybutadienes prepared by lithium-initiated anionic polymerization in nonpolar solvents.[15] Molecular weight distribution was measured by gel permeation chromatography (Waters GPC Model 200). Intrinsic viscosity in tetrahydrofuran at 25 °C was measured by a viscometer in line with the GPC. According to an analysis of these results,[16] the polymers are linear and have narrow distributions ($\bar{M}_w/\bar{M}_n < 1.1$).

Number-average molecular weight was obtained on selected samples by membrane osmometry (Mechrolab Model 501) in toluene at 37 °C. Weight-average molecular weight was obtained by light scattering (FICA 50) in cyclohexane at 25 °C. The summary of characterization data in Table I shows that these values are consistent with the GPC results.

Network Formation and Characterization. Antioxidant was removed from the polymers by dissolving them in toluene and precipitating with methanol. The polymer was then dried under vacuum for at least 1 week. Ten to sixteen samples of each polymer were prepared for irradiation by pressing them gently into plexiglas molds, approximately 1-mm thick, between two 5-mil sheets of mylar. The samples were allowed to relax in the mold for at least 1 week at room temperature under nitrogen. Separate viscoelastic measurements indicated a longest relaxation time of no more than a few hours at 25 °C for even the sample of highest molecular weight. Sixteen samples of one polymer (PB168) in 50% tetradecane solution were also prepared.

The samples in their mylar–plexiglas molds were irradiated in an electron accelerator (Dynamitron, 1.3 MeV) at the Firestone Tire and Rubber Co. The total dose was delivered in nominal increments of $^1/_{10}$, $^1/_4$, 1, or 2 Mrad by repeatedly passing the samples under the scanning electron beam. Dose was measured by the change in optical density of blue cellophane tape. To detect small changes in the flux of electrons an aluminum plate was placed next to the samples and the current generated by the electrons was monitored. Electron energy and sample thickness were such that only the initial, almost linear, part of the depth–dose distribution function was utilized. By a two-sided exposure under these conditions an almost uniform dose density can be obtained.[17]

Some temperature rise occurred in the samples during irradiation. This rise amounted to as much as 30 °C in some cases.

Table II
Elastic and Structural Properties of Networks Formed in the Undiluted State

sample	r, Mrad	t_e,[a] days	$2C_1$, MPa	$2C_2$, MPa	G_0, MPa	$\nu kT/V$, MPa	$(2\nu/\mu)$[b]	T_e
PB096	30.0	15	0.596	0.374	0.970	0.255	4.18	0.617
	42.9	6	0.757	0.411	1.17	0.376	4.26	0.688
	54.2	3	0.895	0.450	1.34$_5$	0.482	4.29	0.723
	65.2	1	1.073	0.439	1.51	0.585	4.31	0.747
	65.2	1	1.074	0.425	1.50	0.585	4.31	0.747
PB168	26.7	20	0.619	0.421	1.04	0.236	4.26	0.703
	32.5	15	0.785	0.404	1.19	0.290	4.30	0.731
	40.3	8	0.825	0.438	1.26	0.363	4.32	0.756
PB210	15.9	15	0.648	0.295	0.94	0.137	4.21	0.651
	18.3	10	0.571	0.418	0.99	0.160	4.25	0.678
	24.0	6	0.630	0.431	1.06	0.213	4.28	0.721
	30.9	3	0.713	0.476	1.19	0.278	4.32	0.752
	30.9	3	0.734	0.465	1.20	0.278	4.32	0.752
PB344	16.2	30	0.668	0.306	0.97	0.144	4.30	0.733
	24.9	12	0.663	0.487	1.15	0.226	4.35	0.779
	32.7	6	0.752	0.471	1.22	0.300	4.37	0.799
	40.8	3	0.821	0.499	1.32	0.376	4.39	0.821
PB725	16.3	30	0.729	0.395	1.12	0.150	4.38	0.803
	24.2	20	0.843	0.389	1.23	0.224	4.40	0.824
	24.6	20	0.836	0.378	1.21	0.227	4.40	0.824
	32.5	3	0.851	0.501	1.35	0.301	4.41	0.834

[a] Approximate equilibration time per reading. [b] Average functionality of elastically active junctions.

However, samples irradiated to the same total dose over longer times, with correspondingly smaller temperature rises, were found to be essentially identical in gel fraction, swelling ratio, and elastic modulus. The effect of dose rate was found generally to be insignificant. No syneresis was found in the solution-cured networks used here. However, some solvent was expelled at still higher doses, and bubbles, presumably hydrogen generated during irradiation, were observed. Those samples were not used in the study.

The gel content was determined by extraction with toluene. Approximately 0.1 g of each network was placed in 100 mL of toluene containing 0.2 g of antioxidant. Five weeks later the supernatant solution was replaced by toluene without antioxidant. It was established that the gel content was not changed by still longer extraction time. One week later the swollen network was weighed and then dried under vacuum until a constant weight was reached. Visually the swelling of the gels was uniform, indicating good cross-linking uniformity and little if any retained orientation from the molding process. The gel curve and swelling data are given elsewhere.[17] The swelling behavior will be the subject of a future publication.

Elastic Measurements. Stress–strain measurements were performed only on the more highly cross-linked samples (doses 16–65 Mrad for the undiluted samples) because of the excessively long time necessary for equilibrium at lower cross-link density. The samples were first restabilized by swelling with an equal weight of toluene containing 0.5% antioxidant, then dried under vacuum for 1 week. Tetradecane was extracted from the solution-cured samples and the samples were reswollen with a paraffinic oil (Sunpar 2280, Sun Oil Co.). Due mainly to the very slow diffusion of oil in the networks it was not convenient to reswell to 50% volume fraction. The volume fraction of polymer during modulus measurement ranged from 0.53 to 0.58.

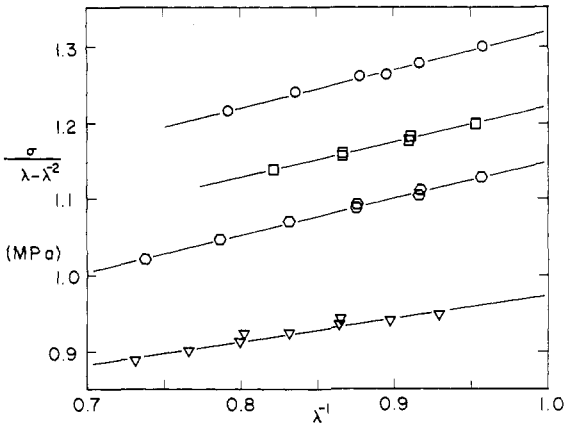

Figure 1. Mooney–Rivlin plots for cross-linked samples of PB344.

Test specimens, 0.25 in. wide and 2 in. long, were cut with a stainless steel die. Two rows of regularly spaced ink dots were drawn on the specimens, and the undeformed cross-sectional area and dot spacings were measured with a Gaertner cathetometer (precision 1 μm). Two grips were attached and the assembly mounted in a plexiglas chamber purged with prepurified nitrogen. Lead weights were hung from the lower grips and the dot spacings were regularly measured with the cathetometer until the deformation was constant. Equilibration at 25 °C required from 1 to 30 days for each load depending on the sample (Tables II and III). The stretch ratio λ was calculated from the equilibrium spacing of dots near the middle of the specimen.

Unloading experiments were performed to test for hysteresis. The difference in equilibrated values of the elongation λ − 1 at the same load was never greater than 0.003 and usually smaller. After testing to break, which required more than 3 months in some cases, the swelling ratio was remeasured in toluene. Changes from initial values were less than 1% in all cases. Fracture usually occurred in the bulk-cured specimens at elongations of 25–40%; elongation at fracture was somewhat larger in the solution-cured networks.

The Mooney–Rivlin form[18]

$$\frac{\sigma}{\lambda - 1/\lambda^2} = 2C_1 + 2C_2/\lambda \tag{5}$$

was used to analyze the data. The values of $\lambda - 1/\lambda^2$ are extremely sensitive to small errors in initial length at small elongations, so we determined the values of $2C_1$ and $2C_2$ in two ways. In the first, the values of λ were calculated with the measured initial dot spacings, and less reliance was placed on the data at small extensions in obtaining $2C_1$ and $2C_2$. In the second, the initial dot spacings were allowed to vary until the best straight line of $\sigma/(\lambda - 1/\lambda^2)$ vs. $1/\lambda$ was obtained. The adjustment required was very small in all cases. The initial modulus

$$G_0 = 2C_1 + 2C_2 \tag{6}$$

was practically the same by either method, although the relative values of $2C_1$ and $2C_2$ were sometimes different. We believe the second method is slightly more reliable, although it does ignore the quite real possibility of slight curvature in Mooney–Rivlin plots. Values obtained by the second method are given in Tables II and III. Examples of Mooney–Rivlin plots (second method)

Table III
Elastic and Structural Properties of Networks Formed from 50% Solutions (PB168S)

r, Mrad	v_2	v_2	t_e, days	$2C_1$, MPa	$2C_2$, MPa	G_0, MPa	$(\nu kT/V^*)-v_2(v_2^0/v_2)^{2/3}$, MPa	$(2\nu/\mu)$	T_e
9.55	0.5	0.562	>30			0.220[a]	0.066	3.96	0.594
16.2	0.5	0.556	>30			0.280[a]	0.098	4.03	0.668
16.2	0.5	0.560	8	0.202	0.113	0.315	0.120	4.06	0.699
20.0	0.5	0.572	3	0.240	0.103	0.343	0.151	4.09	0.730
24.0	0.5	0.582	2	0.269	0.120	0.389	0.184	4.11	0.752

[a] Estimated values, equilibration not quite attained.

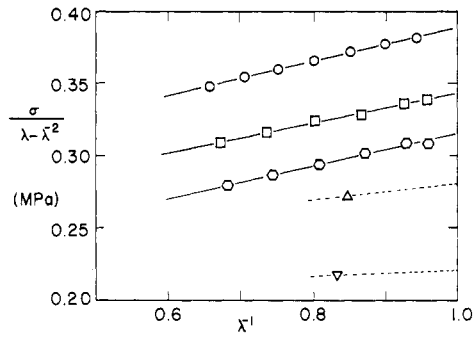

Figure 2. Mooney–Rivlin plots for cross-linked samples of PB168S.

are shown for undiluted networks (PB344) and solution-cured networks (PB168S) in Figures 1 and 2. Only estimated values of G_0 are given for the two solution-cured networks at lower doses because of the excessive time required for equilibration.

Analysis of Gel Curve Data

Pearson et al.[19] have shown that radiation-induced cross-linking of polybutadienes may involve polymerization of vinyl groups to yield some junctions of functionality greater than four. Let $1/i$ be the kinetic chain length of the polymerization–cross-linking reaction and assume termination by coupling (the average functionality of all resulting links is $4/i$). Consider the case of long primary chains which conform to the Schulz–Zimm distribution with number- and weight-average degrees of polymerization y_n and y_w. Let q and p be respectively the fraction of mers which have become part of a cross-link and the fraction which have undergone chain scission. If linking and scission are random the weight fraction of sol w_s can be calculated from the expression[19]

$$w_s = \frac{1}{(\xi + p/q)^3}\left[\frac{2\xi(p/q)(1+\beta)}{\beta q y_w} + (\xi + p/q) \times (p/q)^2 \times - \frac{2\xi(p/q)(1+\beta)}{\beta q y_w}\left(1 + q y_w \frac{\xi + p/q}{1+\beta}\right)^{-\beta} + \xi^2(\xi + p/q)\left(1 + q y_w \frac{\xi + p/q}{1+\beta}\right)^{-(1+\beta)}\right] \quad (7)$$

in which

$$\xi = 1 - w_s i^3[1 - (1 - i)w_s]^{-3} \quad (8)$$

and β is a distribution breadth parameter

$$\beta = \frac{y_n}{y_w - y_n} \quad (9)$$

We assume the extents of linking and scission are directly proportional to radiation dose:

$$q = q_0 r \qquad p = p_0 r \quad (10)$$

Since the samples have similar microstructure the parameters p_0, q_0, and i should be about the same for all samples. Thus the ratio p/q is a constant, and the only dependence on dose occurs in the product $q y_w$. Thus the sol fraction w_s should be a unique function of the product $r\bar{M}_w$ for samples with the same initial distribution breadth.

Figure 3 shows the gelation data plotted in this manner for samples cross-linked in the undiluted state. Values of $\bar{M}_w$ obtained by GPC were used because they are the most accurate relative values. We could find no indication of systematic departures from a single curve, and the increased scatter at low sol fractions is quite understandable

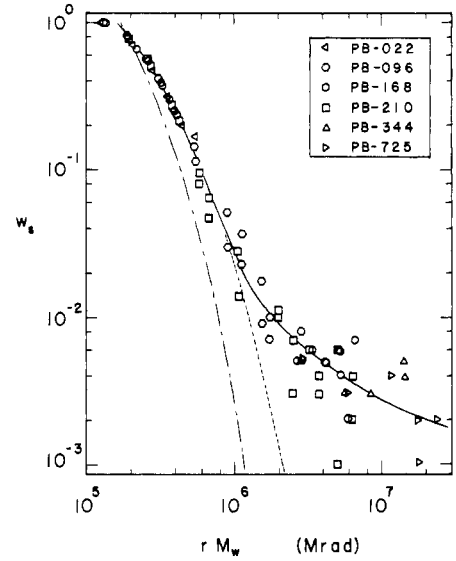

Figure 3. Sol fraction vs. the product of radiation dose and primary chain molecular weight for linear primary chains cross-linked in the bulk. Theoretical curves for multifunctional cross-linking of monodisperse primary chains with scission, $p_0/q_0 = 0.036$ (—); for polydisperse primary chains without scission, $M_w/M_n = 1.1$ (- - -); and for tetrafunctional cross-linking of monodisperse primary chains without scission, (- - -).

from the weighing errors involved.

Values of q_0, p_0/q_0, and i were determined by regression analysis on results from samples PB023, PB096, PB168, and PB210, omitting data at very low sol fractions. Sol fractions ranged from 0.04 to 0.81 and radiation does from 0.9 to 25 Mrad. The parameter β was assumed to be the same for all samples. Minimum deviations were obtained for $\beta = \infty$ (monodisperse primary chains) and

$$q_0 = 2.36 \times 10^{-4}\ \text{Mrad}^{-1} \qquad p_0/q_0 = 0.036 \qquad 4/i = 4.59 \quad (11)$$

If a value $\beta = 10$ was imposed ($\bar{M}_w/\bar{M}_n = 1.1$) the analysis gave virtually the same values of q_0 and $4/i$ but $p_0/q_0 = 0$. The resulting gel curves, together with one calculated for monodisperse primary chains, strictly tetrafunctional linking and no scission, are shown in Figure 3. The low sol data clearly suggest that some chain scission is occurring. These data are in fact fitted rather well by the choice $p_0/q_0 = 0.036$ even when other distribution breadths or modes of linking are assumed.

A similar analysis was applied to sol data ($w_s > 0.1$) for the solution-cured samples. In this case we assume $\beta = \infty$ and $p_0/q_0 = 0.036$ for consistency with the undiluted networks and obtain

$$q_0 = 3.82 \times 10^{-4}\ \text{Mrad}^{-1} \qquad 4/i = 4.37 \quad (12)$$

Figure 4 compares the result with all the solution-cured sol data. The choice $p_0/q_0 = 0.036$ seems reasonably consistent with the low sol data. Curiously, the fraction of mers cross-linked per unit dose is considerably larger in solution than in bulk. Perhaps radicals formed on solvent molecules preferentially transfer to the polymeric double bonds.

Calculation of Network Parameters

Equations developed recently by Pearson and Graessley[20] were used to derive the following expressions:

$$T_e = (1 + w_s - 2\epsilon)^2 \quad (13)$$

$$\nu = qN_0[(1 - \epsilon)(1 - \Theta') - 2(\epsilon - w_s)^2\Theta''] \quad (14)$$

$$\mu = qN_0\left[\frac{i}{2} - \Theta - (1 - w_s)\Theta' - 2(\epsilon - w_s)^2\Theta''\right] \quad (15)$$

$$\epsilon = 1 - \frac{\xi(1+\beta)}{\xi + p/q}\left\{\frac{1}{1+\beta} - \frac{1 - \left[1 + qy_w\frac{\xi + p/q}{1+\beta}\right]^{-\beta}}{\beta qy_w(\xi + p/q)}\right\} \quad (16)$$

$$\Theta = \frac{i^3 w_s^2}{2[1 - (1-i)w_s]^2} \quad (17)$$

$$\Theta' = \frac{i^3 w_s}{[1 - (1-i)w_s]^3} \quad (18)$$

$$\Theta'' = \frac{i^3[1 + 2(i-1)w_s]}{[1 - (1-i)w_s]^4} \quad (19)$$

where N_0 is the number of mers in the network and ξ is defined in eq 8. The values of w_s to be used in these equations are those calculated from eq 7 with the appropriate values of β, q_0, p_0/q_0, and i.

Values of T_e, $\nu kT/V$, and $2\nu/\mu$ (the average functionality of elastically active junctions) were calculated for each of the networks using the density of polybutadiene $\rho = 0.90$ g/cm^3 and $T = 298$ K. The results are given in Table II for the undiluted networks. Values for the solution-cured samples, corrected for volume differences in the case of $\nu kT/V$ (see below), are given in Table III.

Initial Modulus

Samples Cross-Linked in Bulk. The average functionality of active functions, $2\nu/\mu$, varies by less than 5% among the undiluted networks (Table II). Thus, assuming tentatively that the junction fluctuation parameter h also does not vary appreciably among the networks, we can rearrange eq 4 to the form

$$\frac{G_0}{T_e} = A\frac{\nu kT}{VT_e} + G_e^{max} \quad (20)$$

in which $A = 1 - h\mu/\nu$ should be at least approximately a constant.

The data on undiluted networks are plotted according to eq 20 in Figure 5. The points seem to lie along a straight line, and there is no indication of systematic departures related to radiation dose or primary chain molecular weight. The line shown was obtained by a least-squares calculation which yields $A = 1.02$ and $G_e^{max} = 1.18$ MPa. The latter is very close to the reported plateau modulus ($G_N^0 = 1.16$ MPa[10]) although somewhat less than an unpublished result of $G_N^0 = 1.28$ MPa from our laboratory.

Since A is practically unity the average value of h must be quite small, i.e., junction fluctuations are largely suppressed. It is evident, however, that the topological contribution dominates in these networks. The values of G_0 are from 2.5 to 6.5 times larger than $\nu kT/V$, the maximum possible chemical network ($h = 0$) contribution. Thus, small individual variations in h might easily escape attention. This dominance is illustrated in Figure 6 where G_0 is compared with calculated results ($A = 1.02$, $G_e^{max} = 1.18$ Pa) and with $\nu kT/V$ alone.

Samples Cross-Linked in Solution. Since the elastic properties of the solution-cured samples were measured with the network occupying a slightly different volume than the as-formed volume it is necessary to apply small

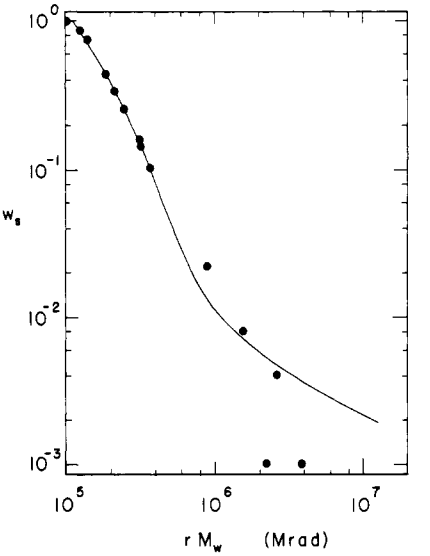

Figure 4. Sol fraction vs. the product of radiation dose and primary chain molecular weight for linear primary chains cross-linked in 50% solution. The theoretical curve is for multifunctional cross-linking of monodisperse primary chains with scission, $p_0/q_0 = 0.036$.

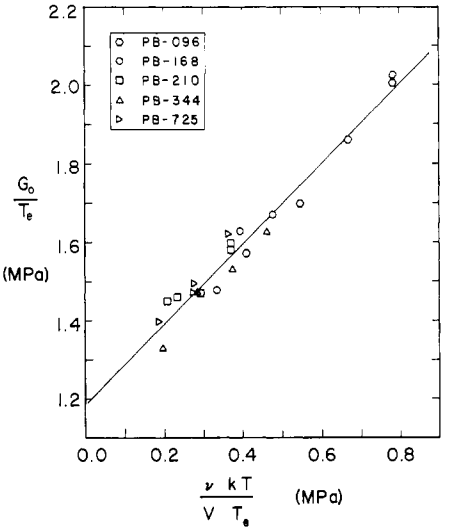

Figure 5. Langley plot for samples cross-linking in the undiluted state.

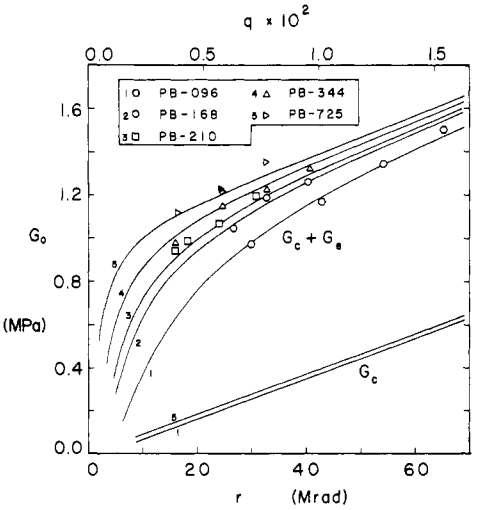

Figure 6. Initial moduli to networks formed by cross-linking in the bulk. The curves were calculated from the network structure with $A = 1.02$ and $G_e^{max} = 1.18$ MPa.

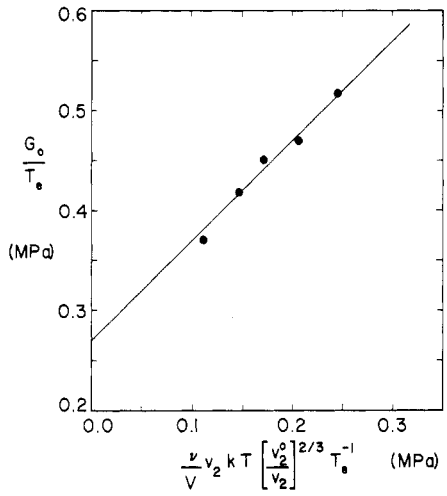

Figure 7. Langley plot for samples cross-linked in 50% solutions (PB168S).

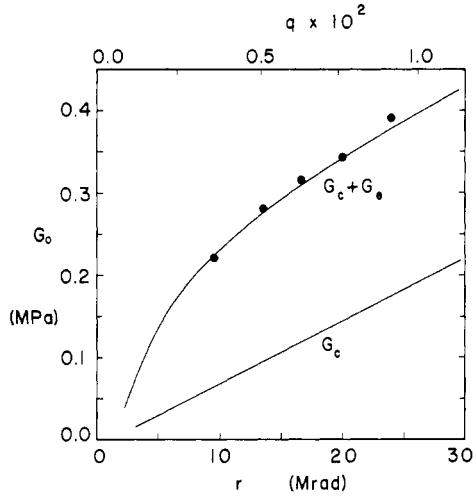

Figure 8. Initial moduli of networks formed by cross-linking calculated from the network structure with $A = 1.0$ and $G_e^{max} = 0.262$ MPa.

corrections to the phantom network term. If V^* is the dry volume of the network and v_2 is the volume fraction of polymer present during modulus measurement the network volume V in eq 1 is V^*/v_2. If v_2^0 is the volume fraction during network formation ($v_2^0 = 0.5$) the ratio $\langle r^2\rangle/\langle r^2\rangle_0$ in eq 1 becomes $(v_2^0/v_2)^{2/3}$. Thus $\nu kTv_2((v_2^0/v_2)^{2/3}/V^*$ (given in Table III) replaces $\nu kT/V$ in eq 20. The net correction for $v_2 \neq v_2^0$ amounts only to a 3–5% adjustment of the values.

Figure 7 shows the resulting Langley plot. A line with slope $A = 1.0$ fits the data well and yields an intercept $(G_e^{max})_{soln} = 0.262$ MPa. This value is close to $(1.18)(0.5)^2 = 0.295$ MPa, calculated from G_e^{max} for the undiluted networks by assuming a quadratic dependence on the volume fraction. It also agrees well with a plateau modulus $(G_N^0)_{soln} = 0.243$ MPa, obtained from measurements on a solution of polybutadiene in tetradecane ($v_2 = 0.48$) which were then adjusted to $v_2 = 0.50$ by assuming quadratic dependence on v_2.

Figure 8 shows the results in relation to the phantom network term ($h = 0$). Since the topological contribution drops rapidly with dilution the differences are not as large as in the undiluted networks, but they are nevertheless still important. The data are fitted well with $A = 1$, implying $h = 0$ and suppressed junction fluctuations as in the undiluted network results. Questions do exist about the effects of small differences from the as-formed volumes in the solution-cured samples and about equilibration in two of the samples. However, we do not believe the uncertainties are large enough to cast any serious doubt on this value of A.

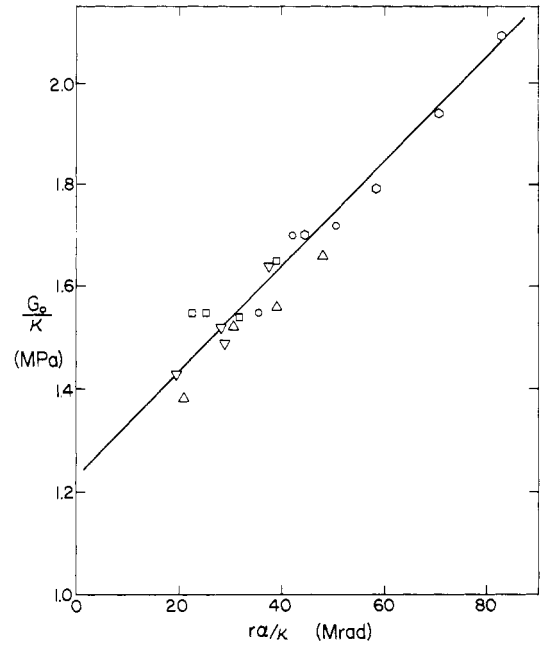

Figure 9. Langley plot for samples cross-linked in bulk with the simplified analysis from eq 21–24.

Results Based on Other Cross-Linking Models. How sensitive are the results to the model used to analyze the gel curve data and calculate the structural parameters of the network? Rather simple equations can be developed for the random tetrafunctional cross-linking of primary chains when there is an average of at least several cross-linked units per primary chain, the primary chain distribution is relatively narrow, and the chain scission frequency is small. The expression for initial modulus can be written

$$G_0 = A\frac{N_0kT}{V}q\alpha + G_e^{max}\kappa \tag{21}$$

in which

$$\alpha = 1 - \delta - 2\delta^2 \tag{22}$$

$$\kappa = (1 - 2\delta)^2 \tag{23}$$

$$\delta = \left(\frac{y_w}{y_n}\right)\frac{1}{qy_w} + p/q \tag{24}$$

and y_w and y_n refer to the primary chains.

From the gel point data on the undiluted samples, $q \approx 2.4 \times 10^{-4}\, r$, and from the sol fractions at large $r\bar{M}_w$, $p/q \approx 0.035$. For the primary chains, $y_w/y_n \approx 1.1$. With this information the values of α and κ can be calculated for each network. A plot of G_0/κ vs. $r\alpha/\kappa$ should yield a line with slope equal to AN_0kTq_0/V and intercept equal to G_e^{max}. Figure 9 shows such a plot for the undiluted networks. The line yields $A = 1.03$ from its slope and $G_e^{max} = 1.23$ MPa from its intercept. Thus, the results are virtually the same as obtained with the more intricate calculations based on polymerization linking and the Schulz–Zimm primary chain distribution. In general the only adjustable parameter which influences the results significantly is p/q, and even if the rather extreme value of $p/q = 0$ is used G_e^{max} only changes to 1.04 MPa and A to 0.94. The results of using still other linking models and parameter choices are given elsewhere,[17] but the conclusions are similar. The

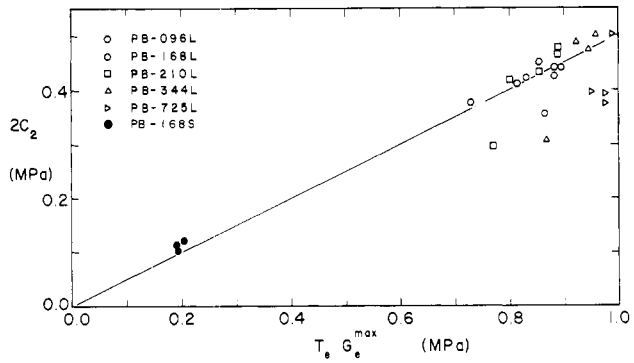

Figure 10. The Mooney–Rivlin parameter $2C_2$ as a function of the entanglement contribution to the initial modulus.

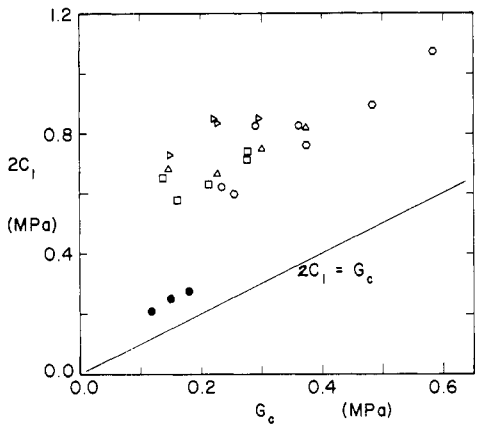

Figure 11. The Mooney–Rivlin constant $2C_1$ as a function of the chemical cross-link contribution to the initial modulus. Symbols are the same as those in Figure 10.

results are insensitive to details of the model.

Finite Deformation Behavior

The molecular origins of departure from neo-Hookean behavior have been a subject of controversy for the past 30 years.[18] We will use the values of $2C_1$ and $2C_2$ obtained here to discuss such behavior, recognizing of course the limitations of the Mooney–Rivlin model in describing general deformations.

In many studies $2C_1$ (the ratio $\sigma/(\lambda - 1/\lambda^2)$ extrapolated to infinite extension) is identified with the chemical (phantom) network contribution, $2C_2$ being in some sense a measure of departure from the molecular theory. Based on a variety of circumstantial evidence, trapped chain entanglements have been suggested as a possible contributor to $2C_2$. The results in this study are consistent with this interpretation. Figure 10 shows $2C_2$ vs. G_e. The line corresponds to

$$2C_2 = \tfrac{1}{2}G_e \tag{25}$$

Some recent results obtained by Macosko[21] on end-linked poly(dimethylsiloxane) networks and Pearson[22] on cross-linked ethylene–propylene copolymers fall close to the same line. Thus, $2C_2$ accounts for approximately half of the topological contribution and, in these studies at least, appears to contain essentially no contribution from the chemical network. It follows that $2C_1$ consists approximately of the entire chemical phantom network contribution G_e plus the other half of the topological contribution:

$$2C_1 = G_c + \tfrac{1}{2}G_e \tag{26}$$

Figure 11 shows $2C_1$ as a function of the phantom network modulus ($h = 0$). The term $2C_1$ clearly contains an appreciable topological component, as has been suggested by Ferry and co-workers.[23]

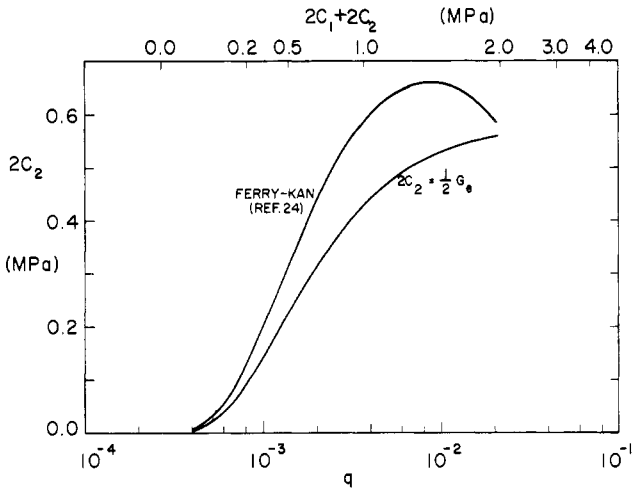

Figure 12. The Mooney–Rivlin parameter $2C_1$ as a function of the fraction of linked mers q for polybutadiene networks.

Figure 12 shows a comparison between the values of $2C_2$ found here (eq 25 and 26) and those calculated from the generalized correlation proposed recently by Ferry and Kan.[24] The differences may be due in part to the limitations of the Mooney–Rivlin form for correlating even tensile data alone. Some gradual curvature in plots of $\sigma/(\lambda - 1/\lambda^2)$ vs. $1/\lambda$ must be expected since smaller slopes are observed in compression, and the behavior should vary smoothly from tension to compression. Our data were limited to relatively small extensions ($1.05 < \lambda < 1.30$), so smaller values of $2C_2$ may have been obtained than that from data at larger extensions which were included in the Ferry–Kan correlation.[24]

Conclusions

We have found that the elastic behavior of a wide variety of polybutadiene networks can be organized around the viewpoint that a topological contribution is present which was trapped permanently in the network when it was formed. Based on this viewpoint, and within the limits of error associated with the two experiments, we have shown that the maximum topological contribution to the initial network modulus, G_e^{max}, is the same as G_N^0, the stress relaxation plateau modulus of the system before cross-linking. This conclusion is drawn only from measurements made on networks occupying their as-formed volumes. Thus, G_e^{max} is 1.18 MPa for a series of undiluted polybutadiene networks and G_N^0 is 1.16 MPa for undiluted polybutadiene, while G_e^{max} is 0.262 MPa for a series formed in 50% solutions ($v_2^0 = 0.5$) and G_N^0 is 0.244 MPa at the same concentration. Both G_e^{max} and G_N^0 are approximately quadratic functions of polymer concentration. It therefore seems inescapable that the same essentially geometrical interactions between chains, interpreted as chain entanglement effects for many years in the case of G_N^0, underlie both properties.

We have also shown that, for these two series of networks at least, the chemical network contribution is equal to that calculated from the phantom network theory with junction fluctuation suppressed. This observation seems to contradict the recent results of Macosko and Valles,[25] who found a chemical contribution in end-linked poly(dimethylsiloxane) networks equal to the phantom network prediction with freely fluctuating junctions ($h = 1$). This difference is possibly related either to the relative magnitude of the topological contribution in the two cases (large in our networks, smaller but still significant in the

Macosko–Valles networks) or to some unsuspected inherent difference in structure between cross-linked and end-linked networks.

Finally, we have observed that the departures from neo-Hookean behavior in these networks are closely associated with the topological contribution. The Mooney–Rivlin parameter $2C_2$ accounts for approximately half the topological contribution to the initial modulus. The parameter $2C_1$ accounts for the other half and appears to include the entire chemical contribution.

Acknowledgment. The authors are grateful to Mr. V. R. Raju and Mr. W. E. Rochefort of this laboratory for providing plateau modulus values and light-scattering molecular weights, to Dr. Georg Böhm and the Firestone Tire and Rubber Co. for providing polybutadiene IR calibration standards and for making the Firestone radiation facility available to us, and to Dr. Gerard Kraus for providing a polybutadiene IR standard. Discussions with Dr. Dale Pearson and Dr. Gary Ver Strate were very helpful throughout. This work was supported by the donors of the Petroleum Research Fund, administered by the American Chemical Society.

Appendix. Asymptotic Expressions for ν, μ, and T_e in Randomly Cross-Linked Networks

Consider a set of long linear chains in which a small fraction of the mer units have been randomly linked. If N_0 is the total number of mers in the system, then N_0q is the number of cross-linked units, $N_0q/2$ is the number of cross-links, and $q \ll 1$. Consider the situation when there is an average of several cross-linked units per chain. In this case the sol fraction will be negligible, nearly all chains will be bound to the network by several links, and nearly all cross-links will have two or more paths leading to the network. Under these conditions the expressions for ν, μ, and T_e become relatively simple.

Consider first the trapping factor T_e. On a chain of n mers the probability that, for the xth mer from one end, there is at least one cross-link somewhere along the chain in each direction (virtually all such cross-links are connected independently to the network under the above conditions) is

$$[1 - (1 - q)^{x-1}][1 - (1 - q)^{n-x+1}] \tag{A1}$$

The fraction of all such mers in n-mer chains is

$$\frac{1}{n}\int_0^n [1 - e^{-qx}][1 - e^{-q(n-x)}]\, dx \tag{A2}$$

in which long chain and small q approximations have been used ($(1 - q)^{x-1} \approx e^{-qx}$, etc.). The result of integration is

$$1 + e^{-qn} - \frac{2}{qn}(1 - e^{-qn}) \tag{A3}$$

and, if the product qn is large enough, we can discard the exponentials to obtain

$$1 - (2/qn) \tag{A4}$$

If $W(n)$ is the fraction of mers contained in n-mers chains (the weight distribution function of the primary chains), the average probability over all chains is

$$\sum_{n=1}^{\infty} W(n)\left(1 - \frac{2}{qn}\right) = 1 - \frac{2}{qy_n} \tag{A5}$$

in which y_n is the number-average degree of polymerization of the chains. If chain scission has taken place along with cross-linking, y_n is related to $(y_n)_0$, the value for the starting polymer, and p, the fraction of mers broken, by

$$\frac{1}{y_n} = \frac{1}{(y_n)_0} + p \tag{A6}$$

The trapping factor is the square of expression A5. Thus, with eq A6

$$T_e = \left[1 - \frac{2}{(y_n)_0 q} - 2p/q\right]^2 \tag{A7}$$

Expressions for the number of elastically active strands and the average functionality of elastically active junctions can be obtained similarly:

$$\nu = \frac{N_0}{V} q\left[1 - \frac{1}{qy_n} - \frac{2}{(qy_n)^2}\right] \tag{A8}$$

$$\bar{f} = 2\frac{\nu}{\mu} = 4\frac{\left[1 - \frac{1}{qy_n} - \frac{2}{(qy_n)^2}\right]}{\left[1 - \frac{8}{(qy_n)^2}\right]} \tag{A9}$$

and eq A6 can be substituted to include chain scission. Departures of eq A7 to A9 from the exact expressions should be small whenever qy_n is large. Equations 21–24 in the text involve simple rearrangements of these equations.

References and Notes

(1) L. R. G. Treloar, "The Physics of Rubber Elasticity", 3rd ed., Clarendon Press, Oxford, 1975.
(2) T. L. Smith, *Treatise Mater. Sci. Technol.*, **10**, 369 (1977).
(3) H. M. James, *J. Chem. Phys.*, **15**, 651 (1947).
(4) A. J. Staverman and J. A. Duiser in "The Physics of Non-Crystalline Solids", J. A. Prins, Ed., North-Holland Publishing Co., Amsterdam, 1965, pp 376–387.
(5) B. Eichinger, *Macromolecules*, **5**, 496 (1972).
(6) W. W. Graessley, *Macromolecules*, **8**, 186, 865 (1975).
(7) P. J. Flory, *Proc. R. Soc. London, Ser. A*, **351**, 351 (1976).
(8) R. G. Kirste, W. A. Kruse, and J. Schelten, *Makromol. Chem.*, **162**, 299 (1972).
(9) G. Jannink et al., *Macromolecules*, **8**, 804 (1975).
(10) J. D. Ferry, "Viscoelastic Properties of Polymers", 2nd ed., Wiley, New York, 1970.
(11) W. W. Graessley, *Adv. Polym. Sci.*, **16**, 1 (1974).
(12) (a) J. Scanlan, *J. Polym. Sci.*, **43**, 501 (1960); (b) G. Ronca and G. Allegra, *J. Chem. Phys.*, **63**, 4990 (1975).
(13) N. R. Langley, *Macromolecules*, 1, 348 (1968).
(14) N. R. Langley and K. E. Polmanteer, *J. Polym. Sci., Polym. Phys. Ed.*, **12**, 1023 (1974).
(15) G. Kraus and K. W. Rollman, *J. Polym. Sci., Polym. Phys. Ed.*, **15**, 385 (1977).
(16) W. S. Park and W. W. Graessley, *J. Polym. Sci., Polym. Phys. Ed.*, **15**, 85 (1977).
(17) L. M. Dossin, Doctoral Dissertation, Northwestern University, 1978.
(18) J. E. Mark, *Rubber Chem. Technol.*, **48**, 495 (1975).
(19) D. S. Pearson, B. J. Skutnik, and G. G. A. Böhm, *J. Polym. Sci., Polym. Phys. Ed.*, **12**, 925 (1974).
(20) D. S. Pearson and W. W. Graessley, *Macromolecules*, 11, 528 (1978).
(21) C. W. Macosko, private communication.
(22) D. S. Pearson, Doctoral Dissertation, Northwestern University, 1978.
(23) R. L. Carpenter, O. Kramer, and J. D. Ferry, *Macromolecules*, **10**, 117 (1977).
(24) J. D. Ferry and H. C. Kan, *Rubber Chem. Technol.*, submitted.
(25) E. M. Valles and C. W. Macosko in "Chemistry and Properties of Crosslinked Polymers", S. S. Labana, Ed., Academic Press, New York, 1977, pp 401–410.